ELSEVIER

Journal of Nuclear Materials 312 (2003) 16–20

journal of nuclear materials

www.elsevier.com/locate/jnucmat

Water formation in graphite and boron-doped graphite under simultaneous O^+ and H^+ irradiation

Allen Y.K. Chen, J.W. Davis, A.A. Haasz *

Fusion Research Group, University of Toronto Institute for Aerospace Studies, 4925 Dufferin Street, Toronto, Ont., Canada M3H 5T6

Received 11 July 2002; accepted 11 October 2002

Abstract

When graphite is exposed to simultaneous irradiation by H^+ and O^+, in addition to the H^+-induced hydrocarbon and O^+-induced CO and CO_2 formation, water is also formed. The present investigation explores the effect of the presence of boron in graphite on water formation. The results show that B-doped graphite specimens (~15 at.% B) exposed to simultaneous O^+ and H^+ irradiation produce less water when compared to pure graphite under similar irradiation. The concept of the formation of 'water-precursors' at the end of the O^+ range is proposed to explain the observed effect.

1. Introduction

Oxygen is often one of the main intrinsic impurities in the plasma of current fusion devices with carbon first walls. Therefore, the synergistic reactions of oxygen-containing ions and the hydrogenic fuel with carbon materials play an important role in the complex process of plasma wall interaction. Our previous investigation of the temperature dependence of chemical erosion yields has demonstrated the formation of water molecules – in addition to hydrocarbons, CO and CO_2 – during simultaneous H^+ and O^+ bombardment of graphite [1]. Also, for the simultaneous H^+ and O^+ irradiation of graphite, small reductions were seen for both the CO and CO_2 yields as compared to the single-species $O^+ \rightarrow C$ case, and for the CH_4 yield as compared to the $H^+ \rightarrow C$ case [1]. Further details of the mechanisms of the interaction between the incident oxygen and hydrogen ions in pure graphite [2] and boron-doped graphite [3] were revealed by varying the energy (i.e., the implantation depth) and flux ratio (Φ_O/Φ_H) of the O^+ and H^+ beams.

For the case of pure graphite, it was found that ion range separation has negligible effect on the H_2O yield, as well as on the reduction of CO, CO_2 and CH_4 formation during O^+–$H^+ \rightarrow C$ reactions, as compared to the $O^+ \rightarrow C$ or $H^+ \rightarrow C$ reactions [2]. The independence of H_2O yield (and the accompanying CO and CO_2 yield reductions) on the energy separation was thought to be caused by the ability of hydrogen atoms to freely travel on internal surfaces in the modified implantation zone to react with the immobile trapped oxygen [2]. Methane reduction was explained by a separate phenomenon: methane molecule break-up due to energetic oxygen bombardment as the CH_4 molecules make their way out of graphite [2,4,5].

The relative changes of CO, CO_2, and CH_4 yields, as well as the H_2O yield, however, do depend on the Φ_O/Φ_H flux ratio in the case of pure graphite. The *reductions* of CO/O^+ and CO_2/O^+ yields during H^+ and O^+ co-bombardment were found to be the largest for 'small' flux ratios ($\Phi_O/\Phi_H \sim 10\%$); the corresponding water yield (H_2O/O^+) was also the largest for the 10% flux ratio case [2]. This was explained by the relatively higher abundance of mobile hydrogen concentration, leading to the formation of water in the small Φ_O/Φ_H

* Corresponding author. Tel.: +1-416 667 7734; fax: +1-416 667 7925.

E-mail address: aahaasz@utias.utoronto.ca (A.A. Haasz).

0022-3115/03/$ - see front matter
PII: S0022-3115(02)01553-2

flux ratio cases [2]. On the other hand, the reductions of CH_4/H^+ yields during H^+ and O^+ co-bombardment, as compared to $H^+ \rightarrow C$ reactions, were seen to be the highest for 'large' ($\Phi_O/\Phi_H \geqslant 30\%$) flux ratios. This was explained by the high concentration of energetic oxygen ions breaking up more methane molecules [2].

Doped graphite provides an interesting opportunity to further examine the mechanisms of the synergistic effect in the O^+–$H^+ \rightarrow C$ interaction described above. Chemical erosion studies with doped graphites under hydrogen ion irradiation showed that hydrocarbon yields could be reduced by the presence of non-carbon dopant elements [6–12]. To explain the observed experimental results of methane formation yields under simultaneous O^+ and H^+ bombardment of B-doped graphite, it was proposed that boron leads to an enhancement of the recombination of mobile hydrogen atoms, which in turn lowers the CH_4 yield through the reduction of the available hydrogen supply [3].

The objective of the present study is to investigate water formation during simultaneous O^+–H^+ irradiation of B-doped carbon (i.e., O^+–$H^+ \rightarrow C/B$). Boron-doped graphite may also reveal further clues to the mechanisms leading to synergistic effects observed in pure graphite.

2. Experiment

Extensive investigations of the chemical erosion of graphite have been performed in our laboratory under conditions of simultaneous bombardment by O_2^+ and H_3^+ ions, using an independently controlled high-flux, low-energy, mass-analyzed dual-beam ion accelerator system, e.g., Refs. [3,13]. Based on results of previous studies of methane formation in graphite under energetic H^+ and H_3^+ irradiation [14], it is assumed that the incident O_2^+ and H_3^+ molecular ions break up immediately into atoms upon impact with the specimen, and act independently within the graphite. Here, we shall refer to the incident particles as H^+ and O^+ even though not all of the atoms in the molecular ions are charged. The experimental setup comprises the O^+ and H^+ beams impacting on the specimen at 21° to the normal, resulting in a 42° beam separation. A schematic of the experimental arrangement is shown in Fig. 1.

For the present study the O^+ beam energy was fixed at 5 keV/O^+, and the H^+ beam energy was varied in the range 0.7–3 keV/H^+. The approximate depth profiles of the O^+ and H^+ beams, based on the energies used, were calculated using the TRVMC program [15] assuming a graphite material doped with 15 at.% boron with a bulk density of ~2000 kg/m^3; see Ref. [3]. The calculated profiles, shown in Fig. 2, are similar to profiles calculated for pure graphite [2]. Hydrogen beam fluxes were in the range 0.6–3.1 × 10^{19} H^+/m^2 s, while the oxygen

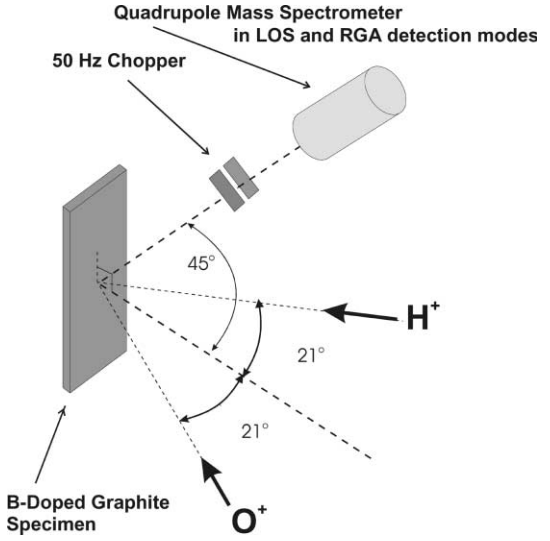

Fig. 1. Schematic diagram of experimental apparatus used for simultaneous H^+ and O^+ irradiation.

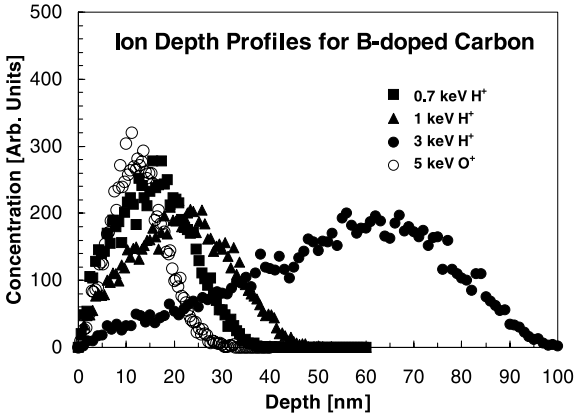

Fig. 2. Implantation depth profiles for H^+ and O^+ in graphite doped with ~15 at.% B. Calculations were performed using the TRVMC code [15].

beam flux was fixed at ~3 × 10^{18} O^+/m^2 s. The resulting flux ratio (Φ_O/Φ_H) was in the rage ~10–50%. The beam spots were slightly elliptical in shape due to off-normal incidence, with *quasi-diameters* of ~5 mm for H^+ and ~3 mm for O^+. This allowed complete frontal overlapping of the O^+ beam spot by the H^+ beam on the specimen. In essence, the same sets of flux/energy dependence experiments described in [2] for pure graphite were performed here for graphite doped with boron.

Two types of boron-doped graphite specimens were used. One was manufactured by Ceramics Kingston Ceramique Inc. (CKC), Canada, using finely ground graphite (10–45 μm) mixed with an organic binder with

boron added as B metal particulates of ~μm size. This material contains about 20 at.% B in the bulk (depth > 1 μm), and about 14 at.% B on the surface (depth < 1 μm). It has a measured density of 1970 kg/m^3. This is the same material that was designated as CKC-B20-base in the experiment described in [6]. For consistency with previous papers, we have retained the CKC-B20 designation even though the relevant B concentration for chemical reactions in the ion implantation zone is the near-surface value of 14 at.% B. The other specimen (USB15) was a fine-grain (~0.01 μm) B-doped graphite manufactured by NII Grafit USSR with a density of ~2000 kg/m^3 and a uniform distribution of 15 at.% B [10]. Both specimens were cut into $25 \times 10 \times 0.5$ mm^3 strips for the irradiation experiments.

The target chamber in which the specimens were housed was baked for at least 24 h at ~500 K before the experiments. The specimens were annealed to >1200 K prior to ion irradiation. Reaction products were measured by quadruple mass spectrometry (QMS) mainly in the residual gas analysis (RGA) mode, after steady-state H_2O production was attained. QMS line-of-sight (LOS) analysis was also performed to detect O and O_2 re-emission, as well as for detecting B_xO_y molecules. A computer controlled data acquisition system was used to collect the QMS data. Although not reported here, in addition to the water QMS signals, the methane, CO and CO_2 signals were also monitored; these results are available in Ref. [3,16]. The absolute erosion yield of water produced by simultaneous H^+ and O^+ irradiation of the test specimens was estimated from the difference of the oxygen balances between single-species $O^+ \rightarrow C/B$ and simultaneous O^+–$H^+ \rightarrow C/B$ cases, based on measured CO and CO_2 yields. This calibration implicitly assumes negligible amounts of B_xO_y molecule formation for both the O^+-only and O^+ and H^+ irradiation cases. This is a reasonable assumption based on an extrapolation of B_xO_y yields, scaled to B content, measured by Vietzke et al. for B_4C due to O^+ impact [17]. Therefore, using the O balance method we get:

$$Y_{H_2O} = (Y_{CO} + 2Y_{CO_2})|^{O^+\text{-only}} - (Y_{CO} + 2Y_{CO_2})|^{O^+ \text{ and } H^+}, \quad (1)$$

where Y_{H_2O}, Y_{CO} and Y_{CO_2} are the H_2O/O^+, CO/O^+, and CO_2/O^+ yields, respectively. The absolute CO and CO_2 erosion yields were obtained using commercially produced calibrated leaks with an absolute error of 20%. For cases where the highest water signals were observed, the yields were estimated using this oxygen balance method, while all other yields were scaled accordingly. The specific cases used for the oxygen balance calibrations were (i) for the CKC-B20 specimen: $\Phi_O/\Phi_H \sim 10\%$, $R_H/R_O \sim 1$ (beams overlapping), and (ii) for the USB15 specimen: $\Phi_O/\Phi_H \sim 50\%$, $R_H/R_O \sim 6$ (beams separated).

3. Results and discussion

As with the $O^+ \rightarrow C$ and O^+–$H^+ \rightarrow C$ irradiation cases, no re-emission of O or O_2 was observed in the LOS detection mode for both the $O^+ \rightarrow C/B$ and O^+–$H^+ \rightarrow C/B$ irradiations of the CKC-B20 and USB15 specimens. Fig. 3 shows the QMS water ($m/e = 18$) signal traces of typical experimental runs in the RGA detection mode for both the O^+–$H^+ \rightarrow C$ and O^+–$H^+ \rightarrow C/B$ cases at 800 K, the temperature at which maximum H_2O production is observed [1,16]. As indicated by the absence of a decrease of the H_2O signal when the O^+ beam is turned off, water production appears to be suppressed for the B-doped graphite (Fig. 3(b) and (d) for range-overlapping and separated cases, respectively) as compared with pure graphite (Fig. 3(a) and (c) for range-overlapping and separated cases, respectively). The apparent difference in the transient behaviours between the two cases when the H^+ beam is turned on is primarily a result of different chamber conditioning.

The effect of B on water formation is further illustrated in Fig. 4 where H_2O yields are compared for the O^+–$H^+ \rightarrow C$ and O^+–$H^+ \rightarrow C/B$ cases as a function of beam flux ratio Φ_O/Φ_H for two ion range separations: (a) beams are depth-wise completely overlapping ($R_H/R_O \sim 1$) and (b) completely separated ($R_H/R_O \sim 4.4$ for pure graphite, and $R_H/R_O \sim 6$ for doped graphite). Two key observations are evident. (i) Water formation for pure graphite – for both range ratio cases – is significant at $\Phi_O/\Phi_H \sim 10\%$, and is negligible (within experimental error) for all other flux ratios. (ii) For the $\Phi_O/\Phi_H \sim 10\%$ case, water yields are suppressed in both the CKC and USB15 B-doped graphite specimens under simultaneous O^+ and H^+ irradiation, compared to the pure graphite case, for both beam range ratios. We also note that the water yield suppression is more pronounced for the USB15 than for the CKC-B20 specimen. Finally, we note an apparent reverse behaviour for the $\Phi_O/\Phi_H \sim 50\%$ case when the beams are depth-wise completely separated, although all the H_2O yields in this case are small and within experimental uncertainties compared to each other.

As in the O^+–$H^+ \rightarrow C$ system, corresponding to the water production during simultaneous O^+ and H^+ irradiation of the B-doped graphite, reductions of CO and CO_2 yields were generally observed [16] compared to the O^+-only irradiation case. In the O^+–$H^+ \rightarrow C/B$ system, there seems to be a shift in the distribution of CO and CO_2 yields (i.e., generally higher CO yields and lower CO_2 yields, compared to the O^+–$H^+ \rightarrow C$ system) while the total number of O atoms contained in the CO and CO_2 molecules is relatively higher than observed for the O^+–$H^+ \rightarrow C$ case, especially for the USB15 specimen [16]. As we are assuming that all incident oxygen leaves the surface as CO, CO_2, or H_2O molecules, an increase in

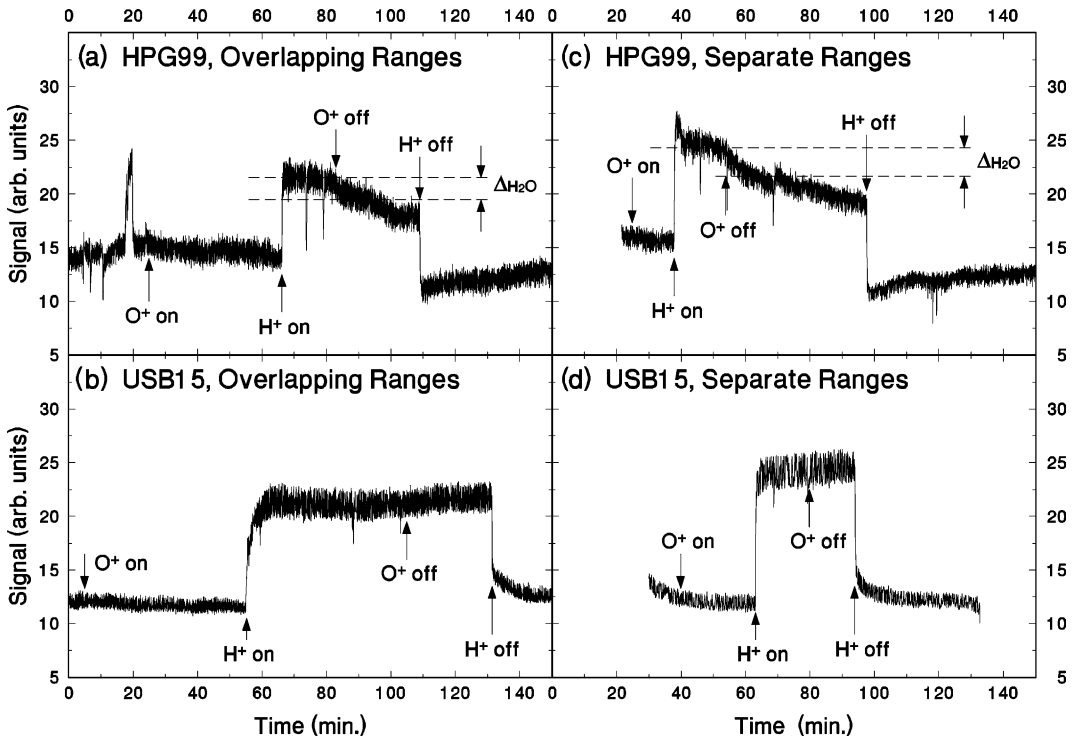

Fig. 3. H_2O QMS (mass 18) signal trace in the RGA detection mode at 800 K for (a) O^+–$H^+ \rightarrow C$ (HPG99) with beam ranges overlapping ($E_O = 5$ keV, $E_H = 0.7$ keV, $\Phi_O \sim 3.0 \times 10^{18}$ O^+/m^2 s) [2], (b) O^+–$H^+ \rightarrow C/B$ (USB15) with beam ranges overlapping ($E_O = 5$ keV, $E_H = 0.7$ keV, $\Phi_O \sim 3.7 \times 10^{18}$ O^+/m^2 s), (c) O^+–$H^+ \rightarrow C$ (HPG99) with beam ranges separated ($E_O = 5$ keV, $E_H = 3$ keV, $\Phi_O \sim 3 \times 10^{18}$ O^+/m^2 s) [2], and (d) O^+–$H^+ \rightarrow C/B$ (USB15) with beam ranges separated ($E_O = 5$ keV, $E_H = 3$ keV, $\Phi_O \sim 3.7 \times 10^{18}$ O^+/m^2 s). The flux ratio Φ_O/Φ_H is about 0.1 for all four traces.

the amount of oxygen contained in CO and CO_2 leads to relatively smaller water yields for the O^+–$H^+ \rightarrow C/B$ system.

Let us now examine the mechanism that causes the water yield reduction for O^+–$H^+ \rightarrow C/B$ as compared to O^+–$H^+ \rightarrow C$. If we assume that during steady-state operation, the *oxygen-gettering* effect of boron reaches a state of saturation, then any effect of boron on the water production must be caused by a change in the chemistry of water production. We postulate the presence of hydrogen-oxygen-containing *complexes* at the end of the O^+ range, created by attaching mobile hydrogen atoms and the implanted oxygen with either carbon or boron on the internal surfaces. The C-attached complexes form the *water-precursor*, which during thermal or ion-induced desorption can release H_2O molecules into internal channels within graphite [16] and transport them out of graphite. The B-attached complexes, on the other hand, have much less probability of releasing H_2O due to the higher stability of the B–O bond. Instead, they may release B_xO_y [17] and H and/or H_2 during thermal or ion-induced desorption. In other words, the presence of boron reduces the H and O supplies by providing competing reaction paths that do not produce water. Since both H and O supplies are reduced by the presence of boron, the flux-dependence effect observed for pure graphite (due to the over-abundance of mobile H supply in the case of $\Phi_O/\Phi_H \sim 10\%$, as discussed in [2]) is reduced. Thus, even at $\Phi_O/\Phi_H \sim 10\%$, H_2O yields were observed to be small for the B-doped graphite, except for the 'anomalous' result (observed in two separate experiments) for the CKC specimen when the H^+ and O^+ beams are depth-wise overlapping; see Fig. 4(a). We attribute this anomalous effect to the relatively coarse grain structure of the CKC specimen in comparison with the much finer grain of the USB15, where the B is much more likely to be uniformly distributed.

The 'water-precursor' *hypothesis* is consistent with the observation of reduced H_2O yield for O^+–$H^+ \rightarrow C/B$ in comparison with O^+–$H^+ \rightarrow C$. Furthermore, it is also consistent with the temperature dependence of water yield [1,16], which suggests the dissociation of the water-precursors at higher temperatures. The 'water-precursor' concept has been incorporated into an 'extended two-region model' for the O^+–$H^+ \rightarrow C$ reaction system [16,18], based on the 'two-region model for hydrogen transport' in Ref. [19].

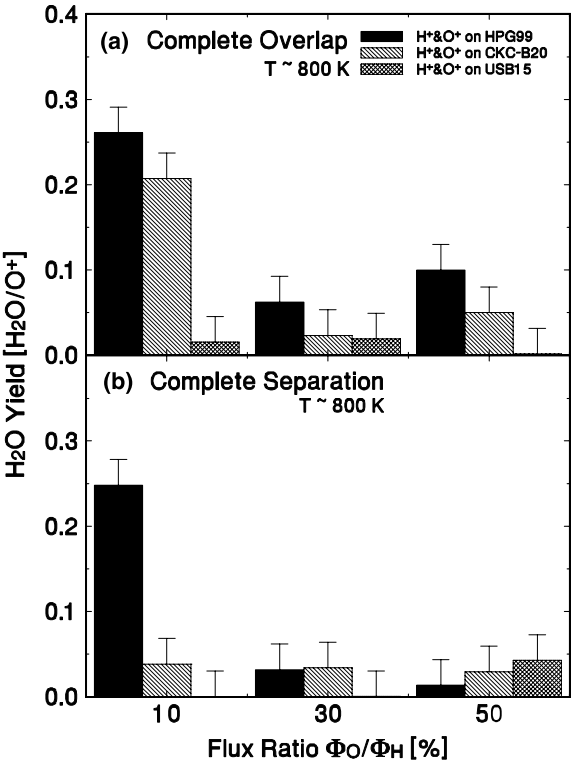

Fig. 4. H_2O yields of both O^+–$H^+ \rightarrow C$ and O^+–$H^+ \rightarrow C/B$ irradiations as a function of beam flux ratio Φ_O/Φ_H for two ion range separation cases: (a) beams are depth-wise completely overlapping, and (b) completely separated. The oxygen flux Φ_O is fixed at $\sim 3 \times 10^{18}$ O^+/m^2 s, while the hydrogen flux Φ_H varies from 0.6–3.1×10^{19} H^+/m^2 s. In the case of O^+–$H^+ \rightarrow C/B$, results are plotted for both CKC-B20 and USB15. All measurements were obtained using QMS–RGA detection. Error bars indicate the relative errors of the yield differences between the single- and dual-beam irradiation cases. The absolute error of the measurement, ~20%, is not included in the error bars.

4. Summary

We have investigated the synergistic interaction occurring during simultaneous H^+ and O^+ irradiation of boron-doped graphite. Similar to our previous studies of pure graphite, we have investigated the effect of varying the ion *range ratio* and *flux ratio* of the two impacting ion species. The results indicate a reduction of water formation for the O^+–$H^+ \rightarrow C/B$ irradiation case when compared to O^+–$H^+ \rightarrow C$. The reduction of water yield due to the presence of boron in the graphite leads to the concept of the formation of 'water-precursors' at the end of the O^+ range, attaching to either carbon or boron atoms. The C-containing OH *complexes* will lead to water formation, while the competing B-containing complexes will contain more stable B–O bonds which will be less likely to produce water. As is the case in pure graphite, the free mobility of H atoms within the implantation zone will allow the H atoms to partake in the water-precursor formation and the subsequent release of water, irrespective of the O^+ and H^+ range separation. Compared to pure graphite, the presence of boron in B-doped graphite reduces both the O and H supply, leading to the suppression of H_2O production even at the $\Phi_O/\Phi_H \sim 10\%$ flux ratio.

Acknowledgements

This work was supported by ITER Canada and the Natural Sciences and Engineering Research Council of Canada. We thank Dr W. Eckstein, IPP-Garching, for making the TRVMC code available for range calculations. We also wish to thank Charles Perez for his help with the preparation of the apparatus.

References

[1] A.A. Haasz, A.Y.K. Chen, J.W. Davis, E. Vietzke, J. Nucl. Mater. 248 (1997) 19.
[2] A.Y.K. Chen, J.W. Davis, A.A. Haasz, J. Nucl. Mater. 266–269 (1999) 399.
[3] A.Y.K. Chen, A.A. Haasz, J.W. Davis, J. Nucl. Mater. 290–293 (2001) 61.
[4] S. Chiu, A.A. Haasz, P. Franzen, J. Nucl. Mater. 218 (1995) 319.
[5] A.A. Haasz, S. Chiu, P. Franzen, J. Nucl. Mater. 220–222 (1995) 815.
[6] A.Y.K. Chen, A.A. Haasz, J.W. Davis, J. Nucl. Mater. 227 (1995) 66.
[7] J. Roth, J. Nucl. Mater. 145–147 (1987) 87.
[8] Y. Hirooka, R. Conn, R. Causey, D. Croessmann, R. Doerner, et al., J. Nucl. Mater. 176&177 (1990) 473.
[9] J.W. Davis, A.A. Haasz, J. Nucl. Mater. 175 (1990) 117.
[10] C. García-Rosales, E. Gauthier, J. Roth, R. Schwörer, W. Eckstein, J. Nucl. Mater. 189 (1992) 1.
[11] A.A. Haasz, J.A. Stephens, E. Vietzke, W. Eckstein, J.W. Davis, Y. Hirooka, in: Atomic and Plasma-Material Interaction Data for Fusion, vol. 7A, 1998.
[12] J. Roth, J. Nucl. Mater. 266–269 (1999) 51.
[13] A.A. Haasz, J.W. Davis, Nucl. Instrum. and Meth. B 83 (1993) 117.
[14] A.A. Haasz, J.W. Davis, O. Auciello, P.C. Stangeby, E. Vietzke, et al., J. Nucl. Mater. 145–147 (1987) 412.
[15] W. Eckstein, TRVMC: vectorized TRIM code for sputtering, multi-component, IPP Garching, FRG, 1993.
[16] A.Y.K. Chen, PhD thesis, University of Toronto, 2001.
[17] E. Vietzke, A. Refke, V. Philipps, M. Hennes, J. Nucl. Mater. 220–222 (1995) 249.
[18] A.Y.K. Chen, A.A. Haasz, J.W. Davis, A semi-empirical model for the O^+–$H^+ \rightarrow C$ reaction system, J. Appl. Phys., submitted for publication.
[19] A.A. Haasz, P. Franzen, J.W. Davis, S. Chiu, C.S. Pitcher, J. Appl. Phys. 77 (1995) 66.